Environmental Microbiome

RESEARCH

Open Access

Effects of drainage and long-term tillage on greenhouse gas fluxes in a natural wetland: insights from microbial mechanisms

Fengqin Liu[1,2], Jiale Yang[2], Wenyan Shen[2], Jiale Fu[3], Jia Meng[1], Yupeng Zhang[1,3*], Jianzheng Li[1*] and Zhiliang Yuan[2*]

Abstract

Background The conversion of natural wetlands to agricultural land through drainage contributes to 62% of the global wetland loss. Such conversion significantly alters greenhouse gas (GHG) fluxes, yet the underlying mechanisms of GHG fluxes resulting from drainage and long-term tillage practices remain highly uncertain. In this study, we measured GHG fluxes of a natural reed wetland (referred to as "Wetland") and a drained wetland that used as farmland (referred to as "Dryland").

Results The results demonstrated that annual cumulative N_2O and CO_2 fluxes in Dryland were 282.77% and 53.79% higher than those in Wetland, respectively. However, CH_4 annual cumulative fluxes decreased from 12,669.45 ± 564.69 kg·ha^{-1} to 8,238.40 ± 207.72 kg·ha^{-1} in Dryland compared to Wetland. The global warming potential (GWP) showed no significant difference between Dryland and Wetland, with comparable average rates of 427.50 ± 48.83 and 422.21 ± 73.59 mg·CO_2-eq·m^{-2}·h^{-1}, respectively. Metagenomic analysis showed a decrease in the abundance of acetoclastic methanogens and their functional genes responsible for CH_4 production. Functional genes related to CH_4 oxidation (*pmoA*) and gene related to N_2O reduction (*nosZ*) exhibited a substantial sensitivity to variations in TOC concentration ($p < 0.05$). *Candidatus* Methylomirabilis, belonging to the NC10 phylum, was identified as the dominant methanotroph and accounted for 49.26% of the methanotrophs. Its relative abundance was significantly higher in Dryland than in Wetland, as the nitrogenous fertilizer applied in Dryland acted as an electron acceptor, with the nearby Wetland produced CH_4 serving as an electron donor. This suggests that Dryland may act as a CH_4 sink, despite the significant enhancement in CO_2 and N_2O fluxes.

Conclusions In conclusion, this study provides insights into the influence of drainage and long-term tillage on GHG fluxes in wetlands and their contribution to global warming.

Highlights

- The flux of N_2O and CO_2 increased, while CH_4 decreased under drainage and tillage.
- Decrease in CH_4 flux offset the component of GWP contributed from N_2O and CO_2.

*Correspondence:
Yupeng Zhang
zhangyp@henau.edu.cn
Jianzheng Li
ljz6677@163.com
Zhiliang Yuan
zhiliangyuan@henau.edu.cn

Full list of author information is available at the end of the article

- The released CH_4 and applicated fertilizer is suitable for DAMO bacteria's growth.
- *Candidatus* Methylomirabilis oxyfera belonging to DAMO is the dominant methanotroph.
- The decrease in abundance of acetoclastic methanogens responsible for CH_4 production.

Keywords Wetland, Greenhouse gas, Drainage, Long-term tillage, Metagenomics

Introduction

As critical carbon reservoirs, wetlands store a minimum of 20% of the global soil organic carbon (SOC) despite covering merely 5% of the Earth's terrestrial surface [1]. The conversion of the vital ecosystem to agricultural land through drainage has emerged as the predominant driver of wetland loss, accounting for 62% of global wetland degradation [2]. However, the process of drainage results in a sudden decrease in water content and a subsequent increase in redox potential, which leads to the rapid loss of carbon (C) and nitrogen (N) in wetlands soil [3, 4]. This loss of soil C and N, in turn, contributes to the production of greenhouse gases (GHGs) such as carbon dioxide (CO_2), methane (CH_4), and nitrous oxide (N_2O), thus contributing global warming. Researches have shown that land use alteration and drainage significantly impact the CH_4 and N_2O as well as CO_2 fluxes [5–7]. Additionally, studies conducted on long-term conservation tillage showed that CO_2 fluxes increased from 900.07 to 924.66 mg CO_2-C kg^{-1} [8]. Similarly, wetland conversion to cropland transformed a CH_4 source of 44.93 ± 10.17 g·CH_4 m^{-2}·yr^{-1} into a small CH_4 sink of -0.056 ± 0.051 g·CH_4 m^{-2}·yr^{-1} [9]. Moreover, a meta-analysis indicated that reclaiming a riparian wetland for cropland increased CO_2 and N_2O fluxes by $54.55 \sim 72.68$ t·ha^{-1} and $2.62 \sim 2.99$ kg·ha^{-1}, respectively [10]. Nevertheless, the mechanistic drivers underlying these GHG flux alterations, specifically the critical interplay between drainage-induced physicochemical changes and long-term agricultural management practices, remain poorly constrained.

Recent research has demonstrated that drainage of wetland significantly disrupts biogeochemical cycles of C and N [11–13]. The impacts are multifaceted, resulting in changes in physicochemical properties of soil as well as the composition and functions roles of microbial communities [14]. These changes subsequently drive the production and consumption of GHGs [10]. The effects of wetland disturbance on GHG fluxes strongly depended on the specific wetland types and disturbance regimes [15, 16]. Moreover, tillage on the drained wetlands resulted in continual and irreversible changes in soil microbial communities. In Yellow River floodplain wetland, ammonia oxidizing and nitrifying bacteria were significantly affected by hydrologic conditions, that significantly influenced microbial catabolism and mineralization of C and N [10, 17]. In the Sanjiang Mire Wetland, proportions of methanotrophic marker genes, i.e., particulate methane monooxygenase (*pMMO*) and soluble methane monooxygenase (*sMMO*) increased by 48.74% and 22.79% following drainage and tillage [9]. Moreover, the decrease in bacterial diversity but increased fungal diversity when wetlands were converted into agricultural land [14, 18, 19]. These changes in microbial communities may lead to the increase in CO_2 and decrease in CH_4 fluxes from the soil [20, 21].

Moreover, the extensive use of fertilizers during tillage has increased the concentration of NO_3^- in soil, providing an electron acceptor for anaerobic methane oxidation by methanotrophs associated with ANME-2d archaea and bacteria of the NC10 phylum. Bacteria of the NC10 phylum exclusively utilize CH_4 as an energy source and are considered critical players in CH_4 reduction through anaerobic methane oxidation pathways [22–24]. These microbes represent a novel microbial CH_4 sink in wetland ecosystems, contributing 9.5%~26.3% of total CH_4 oxidation in tidal flow constructed wetlands [25–27]. *Candidatus* Methylomirabilis oxyfera is the only known functional microbe belonging to the NC10 phylum. Following the conversion of wetlands to farmland, increased concentrations of NO_3^- due to fertilization, as well as significant CH_4 fluxes from surrounding wetlands, providing sufficient substrates for *Candidatus* M. oxyfera and ANME-2d. Hence, it is hypothesized that wetland conversion to farmland increases the abundance of these microorganisms, which then become the primary CH_4 sink, reducing soil GHG fluxes. However, studies exploring the dynamics and contribution of *Candidatus* M. oxyfera and ANME-2d communities during this process are extremely limited.

The Zhalong Wetland is a typical marsh dominated by reeds (*Phragmites communis*), and was listed as a wetland of International Importance in 1992, being ranked first in Asia and fourth globally. Tillage and reclamation have long affected the environment of the Zhalong Wetland. To investigate the effects of drainage and long-term tillage on GHG fluxes, two study sites were selected: Wetland (natural wetland) and Dryland (wetland converted to agricultural land). The aims of this study were: (i) determine the effects of drainage and long-term tillage on soil physicochemical properties and GHG fluxes; (ii) identify shifts in microbial communities and functional genes in response to drainage and long-term tillage; (iii) exploring the dynamics and contributions of *Candidatus* M. oxyfera and ANME-2d communities during drainage and tillage processes, and (iv) explore the mechanisms

through which soil microbial and physio-chemical properties influence GHG fluxes. This study provides a comprehensive assessment of shifts in GHG fluxes across annual cycles in wetlands under drainage and long-term tillage, enabling further evaluation of the implications of agricultural use on wetland ecosystems.

Materials and methods

Study sites

The study sites were selected in the Zhalong wetland (46.867°~47.533°N, 124.229°~124.230°E) located in Heilongjiang province, Northeast China (Fig. 1). The Zhalong wetland is the largest reed wetland in the world, with a total area of approximately 2100 km^2. It has a mid-temperate climate and a mean precipitation of 427 mm [28], which accounts for 61.5% of the total water input [29]. However, imbalanced precipitation and evapotranspiration have led to the conversion of wetland areas into drylands for agricultural purposes. The study sites consisted of an area within the reed wetland (referred to as Wetland) and an adjacent area within the converted dryland, which underwent drainage and long-term tillage (referred to as Dryland). The urea (CH_4N_2O) fertilizer was applied annually in Dryland at a rate of 187.5 $kg{\cdot}ha^{-1}$. No organic amendments or additional phosphorus/potassium fertilizers were used throughout the study period.

Collection and physicochemical analysis of soil samples

In each study site, two layers (0 ~ 20 cm; 20 ~ 40 cm) soil were sampled using a cylindrical stainless-steel soil sampler (Ø 80 mm). Samples were collected from five different plots and combined into one composite sample. All samples were placed in an ice-box and were transferred to the laboratory for microbial and physiochemical analysis. To remove visible plant roots and organic debris, all samples were sieved through a 2-mm mesh screen. After sieving, the samples were divided into two subsamples: the first subsample was used to immediate physicochemical analysis and the second subsample was stored at − 80 °C for DNA extraction and metagenomics sequencing.

After air-drying, soil samples were sieved through a 0.25 mm mesh for physicochemical analysis. The total organic carbon (TOC) and total nitrogen (TN) was measured by an element analyzer (Vario ELcube, Elementar, Germany) [30]. Soil pH was determined by a pH meter (DELTA320, Mettler Toledo, Greifensee, Switzerland) at a soil-to-water mass ratio of 1:2.5 [31]. The concentrations of ammonium nitrogen (NH_4^+) and nitrate nitrogen (NO_3^-) were extracted with 1 $mol{\cdot}L^{-1}$ KCl, and determined by a Lachat flow-injection auto-analyzer (SealAnalytical AA3, Norderstedt, Germany). Three replicates were performed for each sample throughout the experiments.

GHG flux measurement

To measure the GHG flux in two study sites (Fig. 1), the static closed-chamber technique was utilized and three replicative chambers were installed. Each chamber consisted of an upper chamber and a pedestal, with the pedestal inserted into the soil to a depth of 20 cm one month prior to gas sampling. The pedestal gutter was maintained in a water-filled state, and the gas samples were collected 27 times to estimate the annual flux of CO_2, CH_4, and N_2O during study period.

During gas sampling, a 50 mL plastic syringe was used to extract the headspace gas in the chamber [32]. The gas sampling was conducted once every 15 min over a period of 45 min. A 100 mL pre-evacuated gas sampling bag (Delin GasPacking Co., Dalian, China) was used to hold the extracted gas, and the gas samples were immediately transported to the laboratory for gas flux determination. The gas chromatograph (Agilent 7890 A,

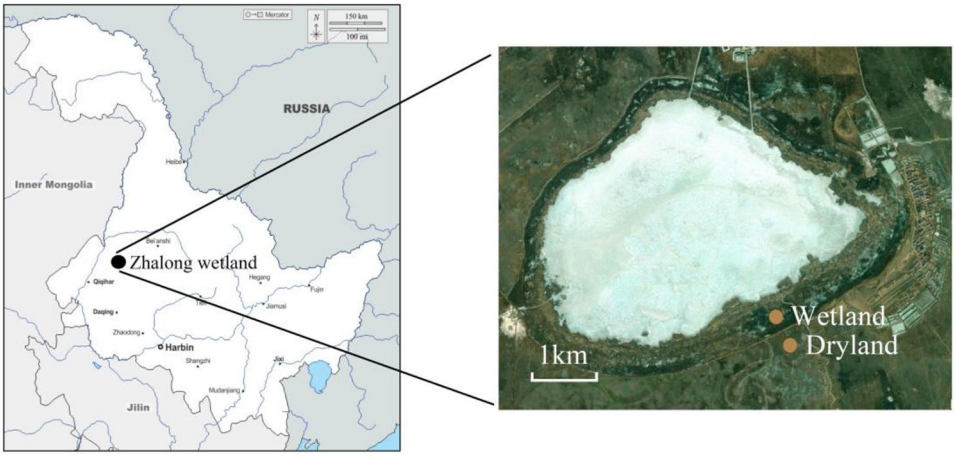

Fig. 1 The location Zhalong wetland (**A**), and the picture (from google earth) shows study site and sample plots (**B**)

Agilent Technologies Inc., Santa Clara, CA, USA) with a methanizer (Ni-catalyst at 350 °C) and a flame ionization detector was used for analyzing CH_4 and CO_2 concentrations. Another gas chromatograph (Shimadzu Analytical and Measuring Instruments Division, Kyoto, Japan) with an electron capture detector was used for determining the concentration of N_2O. With the linear change in gas concentration over the 45 min sampling period was obtained, GHG fluxes (F, $\mu g \cdot m^{-2} \cdot h^{-1}$) were calculated using the method described in ref [29]. The total GWP (global warming potential) for a 100-year horizon in Wetland and Dryland was calculated with [Eq. (1)] [33]. 0

$$\mathrm{GWP_{(Total)}} = \mathrm{Y_{(CO_2)}} + \mathrm{Y_{(CH_4)}} + \mathrm{Y_{(N_2O)}} \quad (1)$$

$$\mathrm{Y_{(CH_4)}} = 27.9 \times \mathrm{Y_{(CO_2)}} \quad (2)$$

$$\mathrm{Y_{(N_2O)}} = 273 \times \mathrm{Y_{(CO_2)}} \quad (3)$$

Where $GWP_{(Total)}$ is total GWP (global warming potential), $Y_{(CO_2)}$, $Y_{(CH_4)}$ and $Y_{(N_2O)}$ indicate the fluxes of CO_2, CH_4 and N_2O, respectively.

The fluxes between every two adjacent intervals of the measurements were used to accumulate cumulative GHG fluxes by the following equation [Eq. (4)] as described previously [34]:

$$\mathrm{E_{cumulative}} = \sum \frac{\mathrm{F_{i+1}} + \mathrm{F_i}}{2} (\mathrm{t_{i+1}} - \mathrm{t_i}) \times 24 \quad (4)$$

Where $E_{cumulative}$ is cumulative GHG fluxes, i means different sampling times and F represents gas flux.

CH4 production and oxidation activity measurement

To determine microbial CH_4 production and oxidation activity, the CH_4 production and oxidation rates were measured with slurry incubation. Briefly, 25 g of sieved soil samples were pre-incubated at 25 °C for 72 h to stabilize the microbial activity in a 250 mL anaerobic glass bottle and divided into 3 groups. In the first group, bottle was sealed with butyl rubber stopper and injected into 10 ml CH_4 (99.9%) to quantify aerobic CH_4 oxidation activity. In the second group, the bottle was flushed with N_2 and sealed with butyl rubber stopper to provide a completely anaerobic environment. This group was used to measure CH_4 production rate. In the third group, the bottle was flushed with N_2 and sealed with butyl rubber stopper, then was injected into 10 ml CH_4 (99.9%) to quantify anaerobic CH_4 oxidation activity [35, 36]. Three replicates were performed for each group. The slurries were incubated for 10 days in a constant temperature incubator at 25 °C. During incubation, the fraction and concentration of headspace gas were measured every day via a gas chromatograph (GC-8850, Shandong Lunan Instrument Factory, China). The chromatograph was equipped with a flame ionization detector (FID) for CH_4 analysis. The gas chromatograph was set up with the split ratio of 1:50.

DNA extraction, metagenomic sequencing and analysis

Genomic DNA was extracted with a DNA SPIN Kit for Soil (MP Biomedicals, USA) according to the manufacturer's instructions. DNA concentration was measured by a NanoDrop 8000 (Thermo Scientific, USA). Metagenomic sequencing was performed on a HiSeq2000 at the Beijing Genomic Institute (ShenZhen, China).

Raw sequences underwent quality control using Trimmomatic (v0.32) [37], and the resulting clean reads were assembled into contigs using SOAPdenovo2 [38] and Rabbit [39]. Contigs with more than 500 base pairs were predicted using MetaGeneMark (v2.10) [40]. Predicted genes were clustered to remove redundant sequences using CD-Hit (with 95% identity and 90% coverage) [41]. Non-redundant genes were compared with the KEGG, eggNOG, and CAZy databases to analyze their functions, and annotation results from various database alignments were obtained.

Statistical analysis

The analysis of variance (ANOVA) was performed to compare differences between samples from Wetland and Dryland by SPSS 25.0 (IBM, USA). One-way ANOVA was used to calculate means and least significant differences at the 5% level. Data visualization was achieved with Origin 2021 (OriginLab, USA). The direct and indirect influence of drainage, long-term tillage, and soil physicochemical characteristics on the GHG fluxes was analyzed using structural equation modeling (SEM) conducted using the semPlot package in R 4.1.0 [42]. The evolutionary tree was made using MEGA 7.0.26 (Mega Limited, Auckland, New Zealand). Mantel test [43] and Pearson's correlation heatmap was conducted by R 4.1.0 using the ggplot2 package [44]. Moreover, abundance heatmaps of microbial communities and functional genes were conducted by pheatmap package of R 4.1.0. Phylogeny of microbial communities and marked genes were visualized by ITOL (Interactive Tree Of Life) v6.0 [45].

Results

Soil physicochemical properties in respond to drainage and long-term tillage

The temporal physicochemical characteristics of soil in Wetland and Dryland were assessed at 10-day intervals from July 2017 to July 2018 (Table 1). The soil pH of Wetland (8.15 ± 0.34) was significantly lower than that of Dryland (8.50 ± 0.27) in 0 ~ 20 cm layer, and the soil pH of Wetland (8.23 ± 0.19) also significantly lower than that of Dryland (8.47 ± 0.21) in 20 ~ 40 cm layer ($p < 0.05$). The

Table 1 Soil properties of Wetland and Dryland in the Zhalong wetland in two layers

	Soil layers	pH	NO_3^--*N* (mg/kg)	NH_4^+-*N* (mg/kg)	TN (g/kg)	TOC (g/kg)
Wetland	0–20 cm	8.15 ± 0.34b	2.76 ± 0.48c	5.86 ± 1.33b	2.06 ± 0.48b	48.94 ± 4.22a
	20–40 cm	8.23 ± 0.19b	2.52 ± 0.39c	3.59 ± 1.01 cd	1.44 ± 0.33b	44.43 ± 3.65b
Dryland	0–20 cm	8.50 ± 0.27a	8.07 ± 1.91a	6.91 ± 2.58a	8.49 ± 1.77a	34.22 ± 3.04c
	20–40 cm	8.47 ± 0.21a	7.11 ± 1.26b	4.78 ± 1.93c	8.04 ± 1.62a	33.86 ± 5.76c

Where data are represented as the mean ($n = 14$) ± standard error (S.E.) and values in each column followed by the different letter are significantly different at $p < 0.05$, symbolizing significant variation of soil properties at different times of the year. NO_3^--N, nitrate nitrogen; NH_4^+-N, ammonium nitrogen; TN, total nitrogen; TOC, total organic carbon

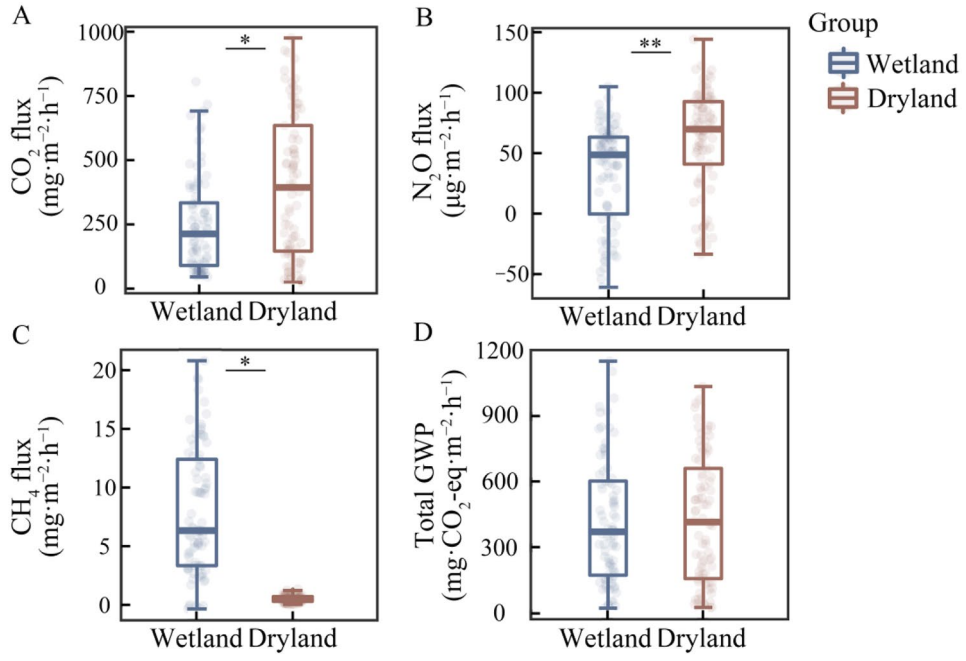

Fig. 2 CO_2 (**A**), N_2O (**B**) and CH_4 (**C**) flux during the study period and total global warming potential calculated for a 100-year horizon (**D**). "*" ($p < 0.05$) and "**" ($p < 0.01$) above the boxes were used to denote significant differences between Wetland and Dryland. GWP: global warming potential

NO_3^--N concentration in Dryland (8.07 ± 1.91 mg·kg^{-1}; 7.11 ± 1.26 mg·kg^{-1}) was significantly higher than that in Wetland (2.76 ± 0.4 mg·kg^{-1}; 2.52 ± 0.39 mg·kg^{-1}) in both 0 ~ 20 cm and 20 ~ 40 cm layer (Table 1, $p < 0.01$). The concentration of NH_4^+-N in 0 ~ 20 cm layer of Dryland soil was 6.91 ± 2.58 mg·kg^{-1}, which was significantly greater than that found in the corresponding layers of Wetland (Table 1, $p < 0.05$). The TOC content in Wetland soil was significantly higher than that in Dryland soil in both layers ($p < 0.05$). However, the concentration of TN in Dryland was significantly elevated compared to Wetland ($p < 0.01$). The differences in soil properties between Wetland and Dryland suggest that long-term drainage of wetlands for agricultural purposes has led to a depletion of the soil's C and N pool.

GHG fluxes and global warming potential following drainage and tillage

GHG fluxes

The fluxes of CO_2, CH_4, and N_2O in both Wetland and Dryland were measured and their cumulative fluxes were calculated (Fig. 2 and Fig. S1). After drainage and long-term tillage, the CO_2 flux of Dryland averaged 398.40 ± 36.50 mg·m^{-2}·h^{-1}, which was significantly higher than that of Wetland (246.47 ± 33.31 mg·m^{-2}·h^{-1}) (Fig. 2A; $p < 0.05$). As a result, the annual cumulative CO_2 flux in Dryland was 12,669.45 ± 564.69 kg·ha^{-1}, which was significantly higher than the corresponding flux (8,238.40 ± 207.72 kg·ha^{-1}) in Wetland (Fig. S1B).

The average CH_4 flux in Wetland was 7.89 ± 1.35 mg·m^{-2}·h^{-1}, which corresponded to 15.29 times that of Dryland (0.52 ± 0.12 mg·m^{-2}·h^{-1}) (Fig. 2C; $p < 0.05$). Furthermore, the annual cumulative CH_4 flux in Wetland (561.88 ± 18.61 kg·ha^{-1}) was significantly higher than that in Dryland (42.97 ± 5.75 kg·ha^{-1}) (Fig. S1C). These results

demonstrated that the drainage and long-term tillage contributed to reduction of CH_4 fluxes in wetlands.

The flux of N_2O were significantly lower in Wetland, with the average of 33.60 ± 9.16 $\mu g \cdot m^{-2} \cdot h^{-1}$ and 61.68 ± 14.67 $\mu g \cdot m^{-2} \cdot h^{-1}$ in Wetland and Dryland, respectively (Fig. 2B; $p < 0.01$). Similarly, the annual cumulative N_2O flux in Dryland (2.98 ± 0.49 $kg \cdot ha^{-1}$) was 4.08 times higher than that in Wetland (0.73 ± 0.20 $kg \cdot ha^{-1}$) (Fig. S1A and B). The annual cumulative fluxes of N_2O decreased from November 15th to March 15th in the subsequent year in both Wetland and Dryland (Fig. S1A), that suggested both sites acted as a N_2O sink in the non-growth season. Thus, N_2O fluxes were significantly increased after drainage and long-term tillage in wetlands.

Activity of methanogenesis and methanotroph

Drainage and long-term tillage significantly suppressed CH_4 production activity in Zhalong wetland soils (Fig. 3A). At a soil depth of 0 ~ 20 cm, the microbial CH_4 production activity of Wetland is 394.89 times higher than that of Dryland, and soil in Dryland exhibited extremely low microbial CH_4 production activity at 20 ~ 40 cm, with the average of 6.03×10^{-4} $\mu g\ C \cdot g^{-1} \cdot d^{-1}$ (Fig. 3A). However, the variation of aerobic CH_4 oxidation activity after wetland drainage was opposite to that of CH_4 production activity (Fig. 3). The CH_4 oxidation activity in Dryland was 1.64 $\mu g\ C \cdot g^{-1} \cdot d^{-1}$, which was significantly higher than that of Wetland (0.45 $\mu g\ C \cdot g^{-1} \cdot d^{-1}$) (Fig. 3B) at 0 ~ 20 cm. The activity of CH_4 oxidation was 1.28 $\mu g\ C \cdot g^{-1} \cdot d^{-1}$, which corresponded to 3.12 times that of Dryland (0.41 $mg \cdot m^{-2} \cdot h^{-1}$) (Fig. 3B). There was no significant difference in anaerobic CH_4 oxidation activity between Wetland and Dryland at 20 ~ 40 cm (Fig. 3C). The anaerobic CH_4 oxidation activity in Dryland (0.35 $\mu g\ C \cdot g^{-1} \cdot d^{-1}$) was remarkably lower than that of Wetland (0.63 $\mu g\ C \cdot g^{-1} \cdot d^{-1}$). Drainage and long-term tillage significantly inhibited CH_4 production activity in Dryland, while enhanced aerobic CH_4 oxidation activity.

Global warming potential

To comprehensively compare the global warming impacts of Wetland and Dryland, we calculated the GWP of the two sites. As shown in Fig. 2D, the GWP of the Dryland was exhibited no significant difference between Wetland and Dryland, with average rate of 427.50 ± 48.83 and 422.21 ± 73.59 $mg \cdot CO_2\text{-}eq \cdot m^{-2} \cdot h^{-1}$, respectively. The largest amount of GWP in Dryland is contributed by CO_2 (93.19%), followed by NO_2 (4.27%), and CH_4 (2.54%). However, in Wetland, the contribution of CH_4 to the GWP was 165.79 ± 113.21 $mg \cdot CO_2\text{-}eq \cdot m^{-2} \cdot h^{-1}$, accounting for 39.27% of the total GWP (Fig. 2D). These findings suggested that total GWP in Dryland contributed from the much lower CH_4 flux had offset that of elevated N_2O and CO_2 fluxes. Thus, it can be inferred that drainage and long-term tillage had no significant impact on total GWP.

Shift in functional genes involved in C-cycling and N-cycling

Microbial functional genes associated with C-cycling were significantly affected by drainage and long-term tillage in the Wetland (Fig. S2A). Functional genes related to CO_2 fixation in Wetland were abundant in both Wetland and Dryland, with the relative abundance of 2.22×10^{-2} and 1.91×10^{-2}, respectively (Fig. S2A). These differences reflect adaptation of the C fixation microbes to changes in environment and substrate availability arising from drainage and long-term tillage of wetland. Functional genes linked to microbial CO_2 production, including fermentation, aerobic respiration, and CO oxidation, showed distinct patterns between Dryland and Wetland (Fig. S2A).

Genes involved in N-cycling were also influenced by drainage and long-term tillage (Fig. S2B). Ammonia oxidation (*amoA*) and denitrification process (*norB*) in soil were the main sources of N_2O. N_2O was then consumed by N_2O reductase (encoded by *nosZ*) in denitrification process. The *nosZ* and *norB* genes were abundant in Wetland compared with Dryland (Fig. S2B). In contrast, *amoA* gene were more abundant in Dryland (Fig.

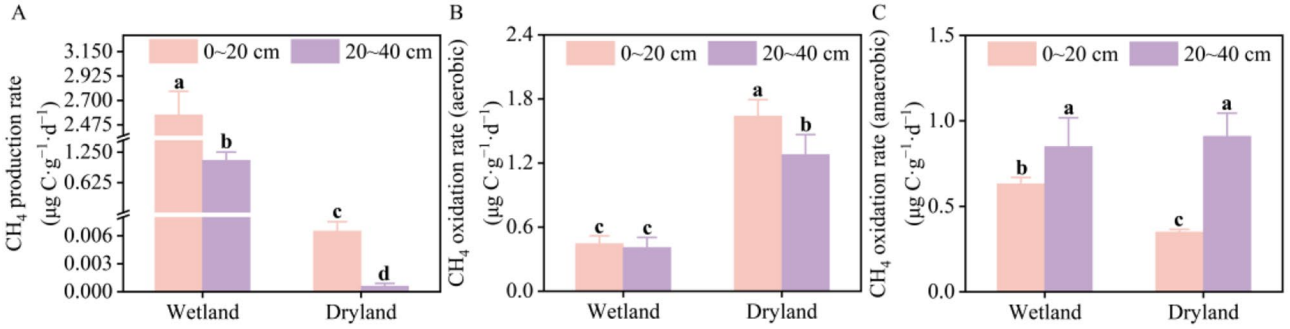

Fig. 3 Microbial anaerobic methane production activity (**A**), aerobic methane oxidation activity (**B**), and anaerobic methane oxidation activity (**C**). Different letters on the bars indicate significant differences ($p < 0.05$)

S2B). These results suggest drainage and long-term tillage decreased the abundance of microbial communities driving both N_2O production and consumption in denitrification process, but increased the N_2O production in ammonia oxidation. Moreover, the tillage increased the abundance of genes participating in urease and nitrogen fixation (Fig. S2B), which implies that the microbial residents of Dryland exhibited a proclivity towards enhancing their capacity to assimilate greater quantities of nutrients from the soil.

During the process of organic matter decomposition, the relative abundance of functional genes involved in starch decomposition were higher in Wetland compared to Dryland, with abundance of 8.94×10^{-4} and 6.78×10^{-4}, respectively (Fig. S3). Similarly, genes related to chitin decomposition were 5.27 times more abundant in Wetland than in Dryland (Fig. S3). In contrast, genes responsible for hemicellulose decomposition exhibited a marked increase from Wetland (6.29×10^{-4}) to Dryland (7.42×10^{-4}). The relative abundance of cellulose decomposition genes in Dryland were 96.22% higher than that in Wetland (Fig. S3). Hence, drainage and long-term tillage promoted the loss of soil resistant C pools though functional genes related to labile carbon decomposition reduced in Dryland which was not enough to offset the SOC loss.

The metabolism of methanogens are the primary microbial source of CH_4 in soil, catalyzing the final step in the anaerobic degradation of SOC [46]. Three methanogenic pathways exist in soil: acetoclastic, methylotrophic, and hydrogenotrophic methanogenesis [47]. In acetoclastic methanogenesis, *Methanosarcina* members utilize phosphate acetyltransferase (*pta*) and acetate kinase (*ackA*) to catalyze reactions that activate acetate to acetyl-CoA. Acetyl-CoA synthetase (*acs*), which also converts acetate to acetyl-CoA, is exclusively found in members of *Methanosaeta* [48]. In Wetland, the relative abundance of *ackA* and *pta* accounted for 60.73% and 67.36% of their total abundance, respectively. Additionally, *acs* had a relative abundance of 1.66×10^{-3} in Wetland, slightly lower than that in Dryland (1.75×10^{-3}) (Fig. 4A). The formyl-MFR synthesis was the first step in hydrogenotrophic methanogenesis, that was catalyzed by formylmethanofuran dehydrogenase (encoded by *fmdA*). The relative abundance of *fmdA* was higher in Dryland (6.58×10^{-5}) compared with that of Wetland (9.36×10^{-6}). Coenzyme M methyltransferase (encoded by *mtaA*) catalyzes the first step of methylotrophic methanogenesis, with a relative abundance of 4.62×10^{-6} in Wetland, while it was not detected in Dryland. The results suggest hydrogenotrophic and acetoclastic methanogenesis were the dominant methanogenic pathways in both Wetland and Dryland.

Aerobic CH_4 oxidation is a microbial metabolic process that generates energy and assimilates carbon from CH_4. It is primarily driven by a specific group of bacteria [49]. The methane monooxygenase (encoded by *pmo*) comprises a diverse group of membrane-bound enzymes, with 80.53% of the *pmo* genes assigned to Dryland (Fig. 4B). As the key enzyme catalyzing $CH_2 = H_4MPT$ synthesis, 5,6,7,8-tetrahydromethanopterin hydro-lyase (*fae*) had a higher relative abundance of 8.52×10^{-5} in Dryland compared with that of Wetland (8.52×10^{-6}) (Fig. 4B). Thus, drainage and long-term tillage stimulated the process of aerobic methane oxidation.

Microbial community dynamics

Acetoclastic methanogens were dominant archaeal community in the Zhalong Wetland with an account of 56.90% in total methanogens (Fig. S4A). Members belonging to acetoclastic methanogens possessed divergent populations at the genus level in Wetland and Dryland. *Methanoculleus*, *Methanobacterium* and *Methanocella* were the most prevalent genera among hydrogenotrophic methanogens (Fig. S4A). The relative abundance of hydrogenotrophic methanogens preferred in the 20 ~ 40 cm layer in both Wetland and Dryland (Fig. S4A), that in line with the functional genes (Fig. 4A). *Methanomethylovorans* was identified in Wetland, and it has the ability to utilize methanol as a substrate [50]. The *Methanomethylovorans* exhibited a relative abundance of 4.09×10^{-3} in the Wetland, which was 2.39 times higher than that observed in the Dryland (Fig. S4A). These results manifested that drainage and long-term tillage significantly increased the relative abundance of acetoclastic methanogens and methylotrophic methanogens, while reduced the populations of hydrogenotrophic methanogens in 0 ~ 20 cm layer.

Methanotrophs were also sensitive to drainage and long-term tillage (Fig. S4B). Members belonging to Methylococcales (Type I) and Rhizobiales (Type II) were identified as typical aerobic methanotrophs [51]. Type II methanotrophs accounted for 88.91% of all aerobic methanotrophs (Fig. S4B). Phylum NC10 and ANME were also found in the soils of the Zhalong Wetland, which were participating in denitrifying anaerobic methane oxidation (DAMO) process. *Candidatus* Methylomirabilis belonging to Phylum NC10 was the dominant methanotrophs that accounted for 49.26% of total methanotrophs and its relative abundance was 9.16% higher in Dryland than that in Wetland (Fig. S4B). Hence, anaerobic methanotrophs served as the primary sink for CH4 in both the Wetland and Dryland.

The community dynamics of key microbes involved in nitrification were analyzed (Fig. S4C). Ammonia-oxidizing archaea (AOA) and ammonia-oxidizing bacteria (AOB) are significant contributors to nitrification and

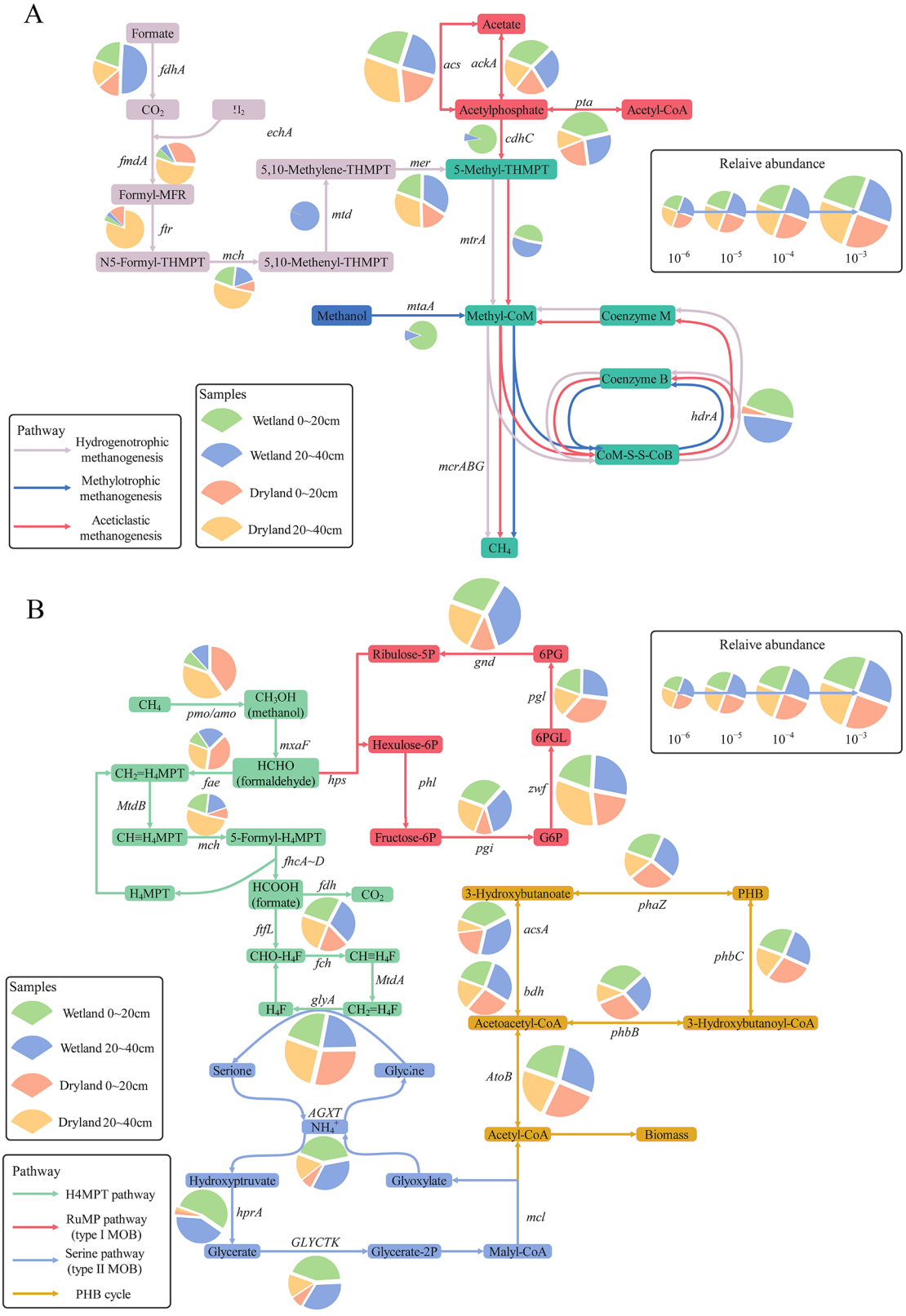

Fig. 4 The methanogenesis (**A**), aerobic methane oxidation (**B**) pathways and relative abundance of functional genes encoding corresponding enzymes. The arrows and blocks with different colors represented specific pathways that were marked. The pies next to the arrow showed the functional genes abundance at 0 ~ 20 cm 20 ~ 40 cm layers in Wetland and Dryland respectively. Abbreviations: PHB, poly-beta-hydroxybutyrate; RuMP: the ribulose monophosphate

nitrogen cycling in soils [52]. AOA were the predominant ammonia oxidizers, constituting 95.35% of the total ammonia oxidizers in Dryland and Wetland (Fig. S4C). The total abundance of AOA in Dryland was 2.05 times greater than that in Wetland. In contrast, AOB were more abundant in Wetland, with a relative abundance 36.57% higher than that in Dryland (Fig. S4C). Among AOB, *Nitrosococcus* and *Nitrosomonas* preferred in Wetland while *Nitrosospira* suitably inhabited in Dryland. These findings suggest that drainage and long-term tillage favored AOA while suppressing AOB.

The abundance of *nosZ* in Wetland were 174.38% higher than that in Dryland (Fig. S5A). This suggests that drainage and long-term tillage restricted N_2O reduction processes. *nosZ* genes can be categorized into clade I and clade II [53]. As depicted in Fig. S5A, 30% of microbes containing the clade II *nosZ* gene were classified under *Flavobacteriia*, while 10.91% of microbes containing the clade I *nosZ* belonged to *Nitriliruptoria*. As a microbial N_2O sink, the quantitative compositions and abundance of *norB* significantly differed between Wetland and Dryland (Fig. S5B). 39.99% of *norB* were affiliated with Gammaproteobacteria, and they were more abundant in Wetland. 19.96% of *norB* were classified under Holophagae, but they were only found in Dryland (Fig. S5B).

Discussion

Linkages between soil properties and GHG fluxes

Soil physicochemical properties and greenhouse gas fluxes exhibited significant variations due to drainage and long-term tillage. Greenhouse gas fluxes were influenced by various complex factors, including SOC quality, temperature, TN, and soil moisture content [54]. The interaction between wetland ecosystems and greenhouse gas emissions exhibits complex dynamics influenced by various factors. Hence, the SEM analysis was employed to distinguish the direct and indirect impacts of drainage, long-term tillage, and soil physicochemical properties on GHG fluxes. Subsequently, significant paths with robust relationships were identified. Specifically, drainage and long-term tillage directly influenced soil pH, TN concentration, and TOC (Fig. 5). The CO_2 fluxes were directly affected by drainage and long-term tillage, and were also influenced by variation of NH_4^+-N level ($p < 0.01$). Notably, a strong positive correlation between NH_4^+-N concentrations and CO_2 fluxes has been observed, which aligns with findings from a study on coastal marshes [55]. The observed NH_4^+-N concentration caused by nitrogen fertilization serves as a key explanatory factor ($r = 0.44$, $p < 0.01$) for the CO_2 flux observed in Dryland (Fig. 5). Furthermore, the CH_4 flux was significantly reduced by drainage and long-term tillage ($p < 0.01$), leading to the lower CH_4 flux observed in Dryland (Fig. 2C). The inhibition roles of drainage on CH_4 flux have been identified in previous studies [9, 56, 57].

Mantel test analysis was then performed to uncover the impact of drainage and long-term tillage on soil physicochemical properties, GHG fluxes, microbial communities, and functional genes. *Gemmatirosa* exhibited significant sensitivity to soil pH ($p < 0.05$), while *Caulobacter* showed notable responsiveness to NO_3^- concentration ($p < 0.05$) (Fig. 6A). The reduction in CH_4 fluxes significantly affected the abundance of *Streptomyces* and *Nitrososphaera* ($p < 0.05$). A robust positive linear correlation exists between NH_4^+-N and N_2O fluxes, which held implications for understanding the elevated N_2O levels observed in Dryland with higher NH_4^+-N content. Similar phenomenon was observed by Zhang and her colleagues, that NH_4^+-N make great contributions to N_2O emission in the North China Plain [58]. The functional genes exhibited higher sensitivity to soil physicochemical properties compared to microbial communities (Fig. 6). Functional genes related to CH_4 oxidation (*pmoA*) and gene related to N_2O reduction (*nosZ*) exhibited a substantial sensitivity to variations in TOC concentration ($p < 0.05$). Genomic evidence has demonstrated a robust correlation between *nosZ* gene abundance and TOC concentration [59]. Conversely, both *fdhB* and *mtaA* genes exhibited notable susceptibility to shifts in pH levels (Fig. 6B).

GHG fluxes in wetlands responded to drainage and long-term tillage

Following drainage and long-term tillage, there was a notable shift in the GHG flux pattern, characterized by elevated CO_2 and N_2O fluxes in Dryland (Fig. 2A and B). This finding aligns with recent research demonstrating the substantial influence of agricultural management practices on GHG fluxes, including factors like additional nitrogen input, TOC, and pH [60]. Distinct tillage practices have also shown to impact GHG fluxes in intermittently flooded paddies [15, 61, 62]. In contrast to the elevated CO_2 and N_2O fluxes, the CH_4 flux experienced a substantial decline from 7.89 ± 1.35 to 0.52 ± 0.12 $mg \cdot m^{-2} \cdot h^{-1}$ following drainage and long-term tillage (Fig. 2C), which was in line with the inhibition of drainage and long-term tillage to CH_4 production activity in Dryland (Fig. S1A). Similar observations have also been made by Wang and her colleagues, who demonstrated that CH_4 emission inhibited after wetland conversion to cropland [9]. On one hand, drainage leads to a rapid reduction in water content and a subsequent rise in redox potential, inhibiting the growth and metabolism of methanogens. On the other hand, the elevated redox potential is conducive to the proliferation of methylotrophs [63]. Hence, the findings support our hypothesis that drainage and long-term tillage can regulate the fluxes of GHGs

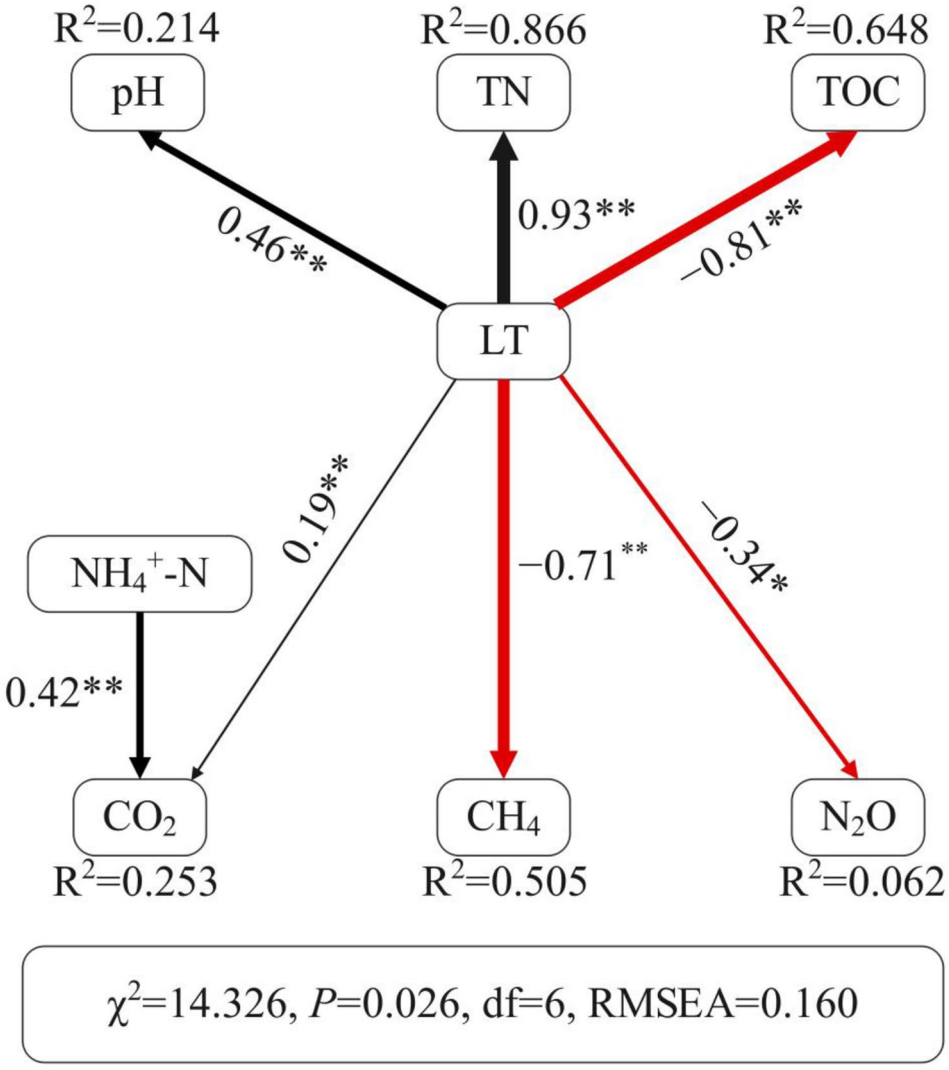

Fig. 5 The structural equation model was used to evaluate direct and indirect influence of long-term tillage on physicochemical properties and greenhouse gas emission. The thickness of arrow appearing in the figure represents the strength of the relationships, additionally, the black arrows and the red arrows indicated positive relationships and negative relationships, respectively. Significance levels were marked: * ($p < 0.05$); ** ($p < 0.01$). Different numbers adjacent to the arrows symbolize standardized path coefficients. NH_4^+-N, ammonium nitrogen; TN, total nitrogen; TOC, total organic carbon

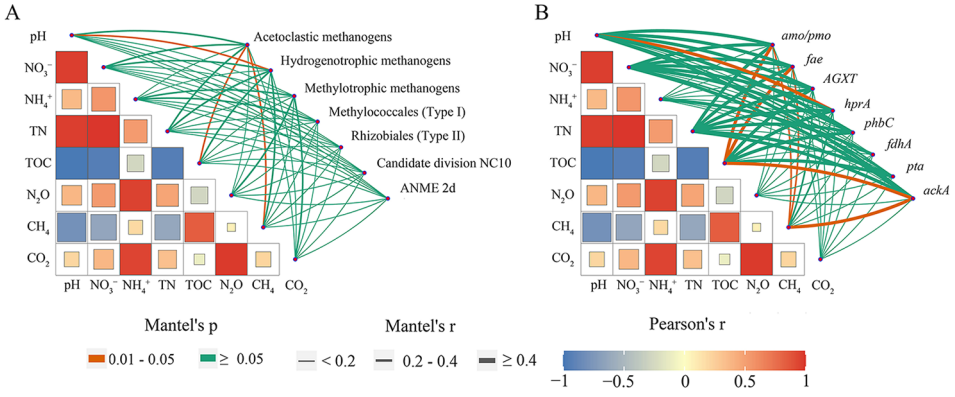

Fig. 6 Mantel test analysis showed the pearson's correlation among soil physicochemical properties and mantel correlation between physicochemical properties and methanogens, methanotrophs, greenhouse gas fluxes (**A**) and abundance of functional genes (**B**), respectively. Annotations: CO_2: CO_2 flux; CH_4: CH_4 flux; N_2O: N_2O flux

(CO_2, CH_4 and N_2O) in wetlands. Nevertheless, despite the notably increased N_2O and CO_2 fluxes observed (Fig. 2D), there was no significant divergence in GWP between Wetland and Dryland. This mainly caused by the decrease in CH_4 flux offset the component of GWP contributed from N_2O and CO_2.

Microbe's response to drainage and long-term tillage

Ammonia oxidation was the first step of nitrification that was dominated by both AOA and AOB [64]. Following drainage and long-term tillage, the relative abundance of ammonia oxidizers increased by 94.87% (Fig. S4C). Nitric oxide reductase (encoded by *norB*) and nitrous oxide reductase (encoded by *nosZ*) play key roles in denitrification [65]. The abundance of *norB* and *nosZ* genes decreased by 63.57% and 20.89% after drainage and long-term tillage (Fig. S5), respectively. This mainly caused by elevated concentrations of oxygen inhibited denitrification processes [66]. Several studies have demonstrated that enhanced soil aeration following drainage, coupled with nitrogen fertilizer application during the transformation of wetlands into agricultural areas, leads to an augmentation in the abundance of ammonia-oxidizing microbes and a reduction in the denitrifying microbial community [67–69]. Moreover, fertilizer application has been shown to enhance N_2O fluxes in cornfields [70, 71]. Hence, drainage and long-term tillage promoted soil nitrification, leading to the inhibition of denitrification in the wetland. This could potentially explain the observed increase in N_2O fluxes.

In comparison to the Wetland, the total abundance of methanogens experienced a notable decrease of 13.55% in the Dryland (Fig. S4A). Conversely, the total abundance of methanotrophs displayed a 13.27% increase in the Dryland (Fig. S4 A and B). Thus, the ratio of methanogens to methanotrophs decreased by 23.67%, which explained the inhibition of drainage and long-term tillage on inhibited CH_4 emission. The ratio of methanogens to methanotrophs has been used as a sensitive indicator for cumulative CH_4 flux in paddy fields [72]. Furthermore, a reduction of 11.46% was observed in the abundance of genes associated with methanogenesis pathways during the transition from Wetland to Dryland (Fig. 4A). Methanogenesis can be classified into three pathways based on their substrate utilization spectrum: CO_2-reducing (hydrogenotrophic), acetate-splitting (aceticlastic), and methyl-reducing (methylotrophic) pathways [73]. Acetoclastic methanogens and hydrogenotrophic methanogens constituted the dominant groups, accounting for 56.90% and 41.67% of the total methanogen abundance, respectively (Fig. S4A). A similar methanogenic pathway was also identified in a wetland and cultivated cropland located in northeastern China [9].

Methanotrophs oxidize CH_4 into CO_2, serving as a crucial microbial sink for CH_4 in wetland soils. Approximately 60%~90% of the CH_4 produced by methanogens in wetland soils undergoes conversion into CO_2 by methanotrophs before released into the atmosphere [74]. The oxidation of CH_4 is carried out by both aerobic methanotrophs and anaerobic methanotrophs [75]. Based on phylogenetic relationships and metabolic characteristics, aerobic methanotrophs can be categorized into two distinct types: Type I and Type II [76]. The total abundance of Type II was significantly higher than that of Type I (Fig. S4B). Type I methanotrophs exhibit a lower affinity for CH_4 and can only utilize CH_4 at concentrations exceeding 40 ppm. On the contrary, Type II methanotrophs exhibit significantly higher affinity for CH_4 compared to Type I methanotrophs. They can utilize CH_4 at concentrations as low as 2 ppm [77]. Members belonging to phylum NC10 and ANME were the dominant anaerobic methanotrophs in both Wetland and Dryland (Fig. S4B). The electron acceptor of these microbes was NO_2^- or NO_3^- during anaerobic oxidation CH_4 [78]. After drainage and long-term tillage, members belonging to phylum NC10 increased 3.87% (Fig. S4B). The Wetland emits a large amount of CH_4, which serves as an electron donor for them [79]. While the concentration NO_3^- of Dryland nearby was also high due to the application of nitrogen fertilizers (Table 1). Sufficient CH_4 and NO_3^- create an optimal habitat for DAMO bacteria in Dryland. This effectively explains the significantly higher anaerobic CH_4 oxidation rate and higher abundance of methanotrophs belonging to the NC10 phylum observed in Dryland (Figs. 3C and 4B).

Conclusion

Drainage and long-term tillage significantly increased soil pH and TN but reduced the concentration of TOC and NH_4^+-N. The flux of N_2O and CO_2 increased, while the CH_4 transitioned from a source to a sink occurred under drainage and long-term tillage. The decrease in CH_4 flux offset the GWP contribution from N_2O and CO_2. The microbial populations of methanogens and methanogenic functional genes were suppressed, whereas the abundance of methanotrophs and microbes involved in N_2O reduction was significantly promoted by drainage and long-term tillage. CH_4 produced in the wetland, along with the application of nitrogenous fertilizer, creates a suitable habitat for *Candidatus* Methylomirabilis oxyfera, which becomes the dominant methanotroph in this environment. The results highlight the influence of drainage

and long-term tillage on GHG fluxes not least in an intense anthropogenic activities context.

Supplementary Information

The online version contains supplementary material available at https://doi.org/10.1186/s40793-025-00682-w.

Supplementary Material 1: Fig. S1 Cumulative fluxes of greenhouse gas involving N2O (A), CO2 (B), and CH4 (C) over the course of a year in Wetland and Dryland. Fig. S2 Heatmap of microbial functional gene related to C-cycling (A) and N-cycling (B) whose abundance was represented as Z-score in Wetland and Dryland. Abbreviations in Fig. A, F: fermentation, R: aerobic respiration; CO: CO oxidation. Abbreviations in Fig. B, A: nitrate ammonification, Nf: nitrogen fixation, M: mineralization, N: ammonia oxidation, O: nitrite oxidation, U: urease. Fig. S3 Heatmap shows the abundance of genes encoding specific enzymes which are related to the degradation of labile and resistant carbon pools in soil. The enzymes shown in the figure can be divided four groups according to different functions: starch degradation (alphaamylase, glucoamylase, neopullulanase II and pullulanase); Cellulose degradation (cellobiase and endoglucanase); Hemicellulose degradation (bacterial arabinofuranosidase, xylose isomerase and xylanase) and Chitin degradation (endochitinase). Fig. S4 The relative abundances of methanogens (A), methanotrophs (B) and ammonia oxidizing communities (C) at the genus level in Wetland and Dryland, respectively. Fig. S5 Phylogeny and relative abundances of nosZ (A) and norB (B) in Wetland and Dryland.

Acknowledgements
We gratefully acknowledge the financial support provided by various institutions and foundations. This research was supported by the Open Project of the State Key Laboratory of Urban Water Resource and Environment at Harbin Institute of Technology, Key Scientific Research Projects of Colleges and Universities, the Natural Science Foundation of Henan, and the Top Talent Foundation of Henan Agricultural University. Their support has been invaluable to the completion of this study.

Author contributions
F.Q. Liu: design of the work. J.L. Yang: wrote the main manuscript text. W.Y. Shen and J.L. Fu: conceived the experiment. J. Meng: data curation. Y. P. Zhang and J.Z. Li: Writing - Review & Editing. Z.L. Yuan: interpretation of data. All authors reviewed the manuscript.

Funding
This research was supported by Open Project of State Key Laboratory of Urban Water Resource and Environment, Harbin Institute of Technology (No. ES202308), China Postdoctoral Science Foundation (No. 2024M763244), Natural Science Foundation of Henan (No. 242300421652), and Top Talent Foundation of Henan Agricultural University (No. 30501300).

Data availability
No datasets were generated or analysed during the current study.

Declarations

Ethics approval and consent to participate
Not applicable.

Consent for publication
Not applicable.

Competing interests
The authors declare no competing interests.

Author details
[1]State Key Laboratory of Urban Water Resource and Environment, School of Environment, Harbin Institute of Technology, Harbin 150090, China
[2]College of Life Sciences, Henan Agricultural University, No.63 Agricultural Road, Zhengzhou 450002, China
[3]College of Resources and Environmental Sciences, Henan Agricultural University, No.63 Agricultural Road, Zhengzhou 450002, China

Received: 27 January 2025 / Accepted: 2 February 2025
Published online: 04 March 2025

References

1. Murray NJ. The extent and drivers of global wetland loss. Nature. 2023;614:234–5. https://doi.org/10.1038/d41586-023-00268-x.
2. Li S, Bush RT, Santos IR, Zhang Q, Song K, Mao R, et al. Large greenhouse gases emissions from China's lakes and reservoirs. Water Res. 2018;147:13–24. https://doi.org/10.1016/j.watres.2018.09.053.
3. Zuber SM, Villamil MB. Meta-analysis approach to assess effect of tillage on microbial biomass and enzyme activities. Soil Biol Biochem. 2016;97:176–87. https://doi.org/10.1016/j.soilbio.2016.03.011.
4. Abraham BS, Caglayan D, Carrillo NV, Chapman MC, Hagan CT, Hansen ST, et al. Shotgun metagenomic analysis of microbial communities from the Loxahatchee nature preserve in the Florida Everglades. Environ Microbiome. 2020;15:2. https://doi.org/10.1186/s40793-019-0352-4.
5. Hoyos-Santillan J, Craigon J, Lomax BH, Lopez OR, Turner BL, Sjögersten S. Root oxygen loss from Raphia taedigera palms mediates greenhouse gas emissions in lowland neotropical peatlands. Plant Soil. 2016;404:47–60. https://doi.org/10.1007/s11104-016-2824-2.
6. Melling L, Hatano R, Goh K. Nitrous oxide emissions from three ecosystems in tropical peatland of Sarawak. Malaysia Soil Sci Plant Nutr. 2007;53:792–805. https://doi.org/10.1111/j.1747-0765.2007.00196.x.
7. Hergoualc'h K, Verchot L. Changes in soil CH_4 fluxes from the conversion of tropical peat swamp forests: a meta-analysis. J Integr Environ Sci. 2012;9:93–101. https://doi.org/10.1080/1943815X.2012.679282.
8. Zhu X, Chang L, Li J, et al. Interactions between earthworms and mesofauna affect CO_2 and N_2O emissions from soils under long-term conservation tillage. Geoderma. 2018;332:153–60. https://doi.org/10.1016/j.geoderma.2017.09.007.
9. Wang N, Zhu X, Zuo Y, Liu J, Yuan F, Guo Z, et al. Microbial mechanisms for methane source-to-sink transition after wetland conversion to cropland. Geoderma. 2023;429:116229. https://doi.org/10.1016/j.geoderma.2022.116229.
10. Lin Q, Wang S, Li Y, Riaz L, Yu F, Yang Q, et al. Effects and mechanisms of land-types conversion on greenhouse gas emissions in the Yellow River floodplain wetland. Sci Total Environ. 2022;813:152406. https://doi.org/10.1016/j.scitotenv.2021.152406.
11. Demirel B, Scherer P. The roles of acetotrophic and hydrogenotrophic methanogens during anaerobic conversion of biomass to methane: a review. Reviews Environ Sci Bio/Technology. 2008;7:173–90. https://doi.org/10.1007/s11157-008-9131-1.
12. Singh S, Chakraborty S. Biochemical treatment of coal mine drainage in constructed wetlands: influence of electron donor, biotic–abiotic pathways and microbial diversity. Chem Eng J. 2022;440:135986. https://doi.org/10.1016/j.cej.2022.135986.
13. Wang B, Liu N, Yang M, et al. Co-occurrence of planktonic bacteria and archaea affects their biogeographic patterns in China's coastal wetlands. Environ Microbiome. 2021;16:19. https://doi.org/10.1186/s40793-021-00388-9.
14. Aguinaga OE, White KN, Dean AP, Pittman JK. Addition of organic acids to acid mine drainage polluted wetland sediment leads to microbial community structure and functional changes and improved water quality. Environ Pollut. 2021;290:118064. https://doi.org/10.1016/j.envpol.2021.118064.
15. Nyamadzawo G, Wuta M, Chirinda N, Mujuru L, Smith JL. Greenhouse Gas emissions from intermittently flooded (Dambo) Rice under different tillage practices in Chiota Smallholder Farming Area of Zimbabwe. Atmospheric Clim Sci. 2013;3:13–20. https://doi.org/10.4236/acs.2013.34A003.
16. Pessi IS, Viitamäki S, Virkkala A-M, Eronen-Rasimus E, Delmont TO, Marushchak ME, et al. In-depth characterization of denitrifier communities across different soil ecosystems in the tundra. Environ Microbiome. 2022;17:30. https://doi.org/10.1186/s40793-022-00424-2.
17. Neupane S, Davis T, Nayduch D, et al. Habitat type and host grazing regimen influence the soil microbial diversity and communities within potential biting

midge larval habitats. Environ Microbiome. 2023;18:5. https://doi.org/10.1186/s40793-022-00456-8.
18. Wang H, Zeng Y, Guo C, Bao Y, Lu G, Reinfelder JR, Dang Z. Bacterial, archaeal, and fungal community responses to acid mine drainage-laden pollution in a rice paddy soil ecosystem. Sci Total Environ. 2018;616–617:107–16. https://doi.org/10.1016/j.scitotenv.2017.10.224.
19. Maus I, Klocke M, Derenkó J, Stolze Y, Beckstette M, Jost C, et al. Impact of process temperature and organic loading rate on cellulolytic / hydrolytic biofilm microbiomes during biomethanation of ryegrass silage revealed by genome-centered metagenomics and metatranscriptomics. Environ Microbiome. 2020;2020(15):7. https://doi.org/10.1186/s40793-020-00354-x.
20. Inglett KS, Inglett PW, Reddy KR, Osborne TZ. Temperature sensitivity of greenhouse gas production in wetland soils of different vegetation. Biogeochemistry. 2011;108:77–90. https://doi.org/10.1007/s10533-011-9573-3.
21. Agethen S, Sander M, Waldemer C, et al. Plant rhizosphere oxidation reduces methane production and emission in rewetted peatlands. Soil Biol Biochem. 2018;125:125–35. https://doi.org/10.1016/j.soilbio.2018.07.006.
22. Henckel T, Roslev P, Conrad R. Effects of O_2 and CH_4 on presence and activity of the indigenous methanotrophic community in rice field soil. Environ Microbiol. 2000;2 6:666–79. https://doi.org/10.1046/j.1462-2920.2000.00149.x.
23. Ettwig KF, Butler MK, Le Paslier D, Pelletier E, Mangenot S, Kuypers MM, et al. Nitrite-driven anaerobic methane oxidation by oxygenic bacteria. Nature. 2010;464:543–8. https://doi.org/10.1038/nature08883.
24. Hu B, Shen L, Lian X, Zhu Q, Liu S, Huang Q, et al. Evidence for nitrite-dependent anaerobic methane oxidation as a previously overlooked microbial methane sink in wetlands. Proc Natl Acad Sci. 2014;111:4495–500. https://doi.org/10.1073/pnas.1318393111.
25. Yang W, Shen L, et al. Role and regulation of anaerobic methane oxidation catalyzed by NC10 bacteria and ANME-2d archaea in various ecosystems. Environ Res. 2023;219:115174. https://doi.org/10.1016/j.envres.2022.115174.
26. Xie F, Ma A, Zhou H, Liang Y, Yin J, Ma K, et al. Niche differentiation of denitrifying anaerobic methane oxidizing bacteria and archaea leads to effective methane filtration in a tibetan alpine wetland. Environ Int. 2020;140:105764. https://doi.org/10.1016/j.envint.2020.105764.
27. Zhang M, Huang J, Sun S, et al. Depth-specific distribution and significance of nitrite-dependent anaerobic methane oxidation process in tidal flow constructed wetlands used for treating river water. Sci Total Environ. 2020;716:137054. https://doi.org/10.1016/j.scitotenv.2020.137054.
28. Weize W, Peng H, Zefan Y, Jianhua W, Jianshi Z, Qinghui Z, et al. Prediction of NDVI dynamics under different ecological water supplementation scenarios based on a long short-term memory network in the Zhalong Wetland, China. J Hydrol. 2022;608. https://doi.org/10.1016/j.jhydrol.2022.127626.
29. Liu F, Zhang Y, Liang H, Gao D. Long-term harvesting of reeds affects greenhouse gas emissions and microbial functional genes in alkaline wetlands. Water Res. 2019;164:114936. https://doi.org/10.1016/j.watres.2019.114936.
30. Chatterjee A, Lal R, Wielopolski L, Martin M, Ebinger M. Evaluation of different Soil Carbon determination methods. CRC Crit Rev Plant Sci. 2009;28:164–78. https://doi.org/10.1080/07352680902776556.
31. Miller R, Kissel D. Comparison of Soil pH methods on soils of North America. Soil Sci Soc Am J. 2010;74. https://doi.org/10.2136/sssaj2008.0047.
32. Murphy RM, Saunders M, Richards KG, Krol DJ, Gebremichael AW, Rambaud J, et al. Nitrous oxide emission factors from an intensively grazed temperate grassland: a comparison of cumulative emissions determined by eddy covariance and static chamber methods. Agric Ecosyst Environ. 2022;324:107725. https://doi.org/10.1016/j.agee.2021.107725.
33. Kamran M, Yan Z, Ahmad I, Jia Q, Ghani MU, Chen X, et al. Assessment of greenhouse gases emissions, global warming potential and net ecosystem economic benefits from wheat field with reduced irrigation and nitrogen management in an arid region of China. Agric Ecosyst Environ. 2023;341:108197. https://doi.org/10.1016/j.agee.2022.108197.
34. Ding W, Cai Y, Cai Z, et al. Nitrous oxide emissions from an intensively cultivated maize–wheat rotation soil in the North China Plain. Sci Total Environ. 2007;373:501–11. https://doi.org/10.1016/j.scitotenv.2006.12.026.
35. Akhtar H, Lupascu M, Sukri RS. Interactions between microtopography, root exudate analogues and temperature determine CO_2 and CH_4 production rates in fire-degraded tropical peat. Soil Biol Biochem. 2022;169:108646. https://doi.org/10.1016/j.soilbio.2022.108646.
36. Yi SC, Heijbroek A, Cutz L, Pillay S, et al. Effects of fir-wood biochar on CH_4 oxidation rates and methanotrophs in landfill cover soils packed at three different proctor compaction levels. Sci Total Environ. 2024;907:167951. https://doi.org/10.1016/j.scitotenv.2023.167951.
37. Bolger A, Lohse M, Usadel B. Trimmomatic: a flexible trimmer for Illumina sequence data. Bioinformatics. 2014;30:2114–20. https://doi.org/10.1093/bioinformatics/btu170.
38. Luo R, Liu B, Xie Y, Li Z, Huang W, Yuan J, et al. SOAPdenovo2: an empirically improved memory-efficient short-read de novo assembler. Gigascience. 2012;1:2047–217. https://doi.org/10.1186/s13742-015-0069-2.
39. You M, Yue Z, He W, Yang X, Yang G, Xie M, et al. A heterozygous moth genome provides insights into herbivory and detoxification. Nat Genet. 2013;45:220–5. https://doi.org/10.1038/ng.2524.
40. Zhu W, Lomsadze A, Borodovsky M. Ab initio gene identification in metagenomic sequences. Nucleic Acids Res. 2010;38:e132–132. https://doi.org/10.1093/nar/gkq275.
41. Godzik LA. Cd-hit: a fast program for clustering and comparing large sets of protein or nucleotide sequences. Bioinformatics. 2006;22:1658. https://doi.org/10.1093/bioinformatics/btl158.
42. Nan Q, Hu S, Qin Y, Wu W. Methane oxidation activity inhibition via high amount aged biochar application in paddy soil. Sci Total Environ. 2021;796:149050. https://doi.org/10.1016/j.scitotenv.2021.149050.
43. Ten-Doménech I, Moreno-Torres M, Castell JV, Quintás G, Kuligowski J. Extracting consistent biological information from functional results of metabolomic pathway analysis using the Mantel's test. Anal Chim Acta. 2021;1187:339173.
44. Gu J, Pitz M, Breitner S, Birmili W, von Klot S, Schneider A, et al. Selection of key ambient particulate variables for epidemiological studies — Applying cluster and heatmap analyses as tools for data reduction. Sci Total Environ. 2012;435–436:541–50. https://doi.org/10.1016/j.scitotenv.2012.07.040.
45. Letunic I, Bork P. Interactive tree of life (iTOL) v5: an online tool for phylogenetic tree display and annotation. Nucleic Acids Res. 2021;49:W293–6. https://doi.org/10.1093/bioinformatics/btl529.
46. Vincent SGT, Jennerjahn T, Ramasamy K. Chapter 3 - environmental variables and factors regulating microbial structure and functions. Microb Communities Coastal Sediments. 2021;79–117. https://doi.org/10.1016/B978-0-12-815165-5.00003-0.
47. Mobilian C, Craft CB. Wetland soils: physical and Chemical Properties and biogeochemical processes. In Encyclopedia of Inland Waters. (Second Edition). 2022;157–68. https://doi.org/10.1016/B978-0-12-819166-8.00049-9.
48. Jetten MSM, Stams AJM, Zehnder AJB. Methanogenesis from acetate: a comparison of the acetate metabolism in Methanothrix soehngenii and Methanosarcina spp. FEMS Microbiol Lett. 1992;88:181–97. https://doi.org/10.1016/0378-1097(92)90802-U.
49. Li J, Liu C, Wu N, et al. Identification of functionally active aerobic methanotrophs and their methane oxidation potential in sediments from the Shenhu Area, South China Sea. China Geol. 2022;5:285–92. https://doi.org/10.31035/cg2022011.
50. Conrad R. Importance of hydrogenotrophic, aceticlastic and methylotrophic methanogenesis for methane production in terrestrial, aquatic and other anoxic environments: a mini review. Pedosphere. 2020;30:25–39. https://doi.org/10.1016/S1002-0160(18)60052-9.
51. Op den Camp HJ, Islam T, Stott MB, Harhangi HR, Hynes A, Schouten S, et al. Environmental, genomic and taxonomic perspectives on methanotrophic Verrucomicrobia. Environ Microbiol Rep. 2009;1:293–306. https://doi.org/10.1111/j.1758-2229.2009.00022.x.
52. Huang L, Chakrabarti S, Cooper J, et al. Ammonia-oxidizing archaea are integral to nitrogen cycling in a highly fertile agricultural soil. ISME Commun. 2021;1:19. https://doi.org/10.1038/s43705-021-00020-4.
53. Hallin S, Philippot L, Löffler FE, Sanford RA, Jones CM. Genomics and Ecology of Novel N_2O-Reducing microorganisms. Trends Microbiol. 2018;26:43–55. https://doi.org/10.1016/j.tim.2017.07.003.
54. Liu X, Lu X, Yu R, Sun H, Xue H, Qi Z, et al. Greenhouse gases emissions from riparian wetlands: an example from the Inner Mongolia grassland region in China. Biogeosciences. 2021;18:4855–72. https://doi.org/10.5194/bg-18-4855-2021.
55. Tan L, Zhang L, Yang P, et al. Effects of conversion of coastal marshes to aquaculture ponds on sediment anaerobic CO_2 production and emission in a subtropical estuary of China. J Environ Manage. 2023;338:117813. https://doi.org/10.1016/j.jenvman.2023.117813.
56. He H, Zhang T, Yao Y, Yang W, Busayo D, Wen X, et al. Tillage Methods on Greenhouse Gas Emissions and yields of Rice–Wheat Rotation System in East China Polder Area. Int J Plant Prod. 2021;15:485–98. https://doi.org/10.1007/s42106-021-00152-6.

57. Zhang H, Bai X, Xue J, Chen Z, et al. Emissions of CH_4 and N_2O under different Tillage systems from double-cropped Paddy Fields in Southern China. PLoS ONE. 2013;8:e65277. https://doi.org/10.1371/journal.pone.0065277.
58. Zhang Y, Guo G, Wu H, Mu Y, Liu P, Liu J, Zhang C. The coupling interaction of NO_2^- with NH_4^+ or NO_3^- as an important source of N_2O emission from agricultural soil in the North China Plain. Sci Total Environ. 2019;692:82–8. https://doi.org/10.1016/j.scitotenv.2019.07.244.
59. Qi C, Zhou Y, Suenaga T, Oba K, Lu J, Wang G, et al. Organic carbon determines nitrous oxide consumption activity of clade I and II nosZ bacteria: genomic and biokinetic insights. Water Res. 2022;209:117910. https://doi.org/10.1016/j.watres.2021.117910.
60. Chen M, Chang L, Zhang J, Guo F, Vymazal J, He Q, Chen Y. Global nitrogen input on wetland ecosystem: the driving mechanism of soil labile carbon and nitrogen on greenhouse gas emissions. Environ Sci Ecotechnol. 2020;4:100063. https://doi.org/10.1016/j.ese.2020.100063.
61. Alhassan AM, Yang C, Ma W, Li G. Influence of conservation tillage on Greenhouse gas fluxes and crop productivity in spring-wheat agroecosystems on the Loess Plateau of China. PeerJ. 2021;9:e11064. https://doi.org/10.7717/peerj.11064.
62. Bhattacharyya SS, Leite FFGD, France CL, Adekoya AO, Ros GH, de Vries W, et al. Soil carbon sequestration, greenhouse gas emissions, and water pollution under different tillage practices. Sci Total Environ. 2022;826:154161. https://doi.org/10.1016/j.scitotenv.2022.154161.
63. Chistoserdova L. Methylotrophs in natural habitats: current insights through metagenomics. Appl Microbiol Biotechnol. 2015;99:5763–79. https://doi.org/10.1007/s00253-015-6713-z.
64. Gao D, Liu F, Xie Y, Liang H. Temporal and spatial distribution of ammonia-oxidizing organisms of two types of wetlands in Northeast China. Appl Microbiol Biotechnol. 2018;102:7195–205. https://doi.org/10.1007/s00253-018-9152-9.
65. Braker G, Tiedje JM. Nitric oxide reductase (*norB*) genes from pure cultures and environmental samples. Appl Environ Microbiol. 2003;69:3476–83. https://doi.org/10.1128/AEM.69.6.3476-3483.2003.
66. Pan B, Xia L, Lam SK, Wang E, Zhang Y, Mosier A, Chen D. A global synthesis of soil denitrification: driving factors and mitigation strategies. Agric Ecosyst Environ. 2022;327:107850. https://doi.org/10.1016/j.agee.2021.107850.
67. Wu L, Chen X, Wei W, Liu Y, Wang D, Ni BJ. A critical review on Nitrous Oxide production by Ammonia-Oxidizing Archaea. Environ Sci Technol. 2020;54:9175–90. https://doi.org/10.1021/acs.est.0c06792.
68. Guo H, Ma L, Liang Y, Hou Z, Min W. Response of ammonia-oxidizing Bacteria and Archaea to long-term saline water irrigation in alluvial grey desert soils. Sci Rep. 2020;10:489. https://doi.org/10.1038/s41598-019-57402-x.
69. Nie Sa, Zhu G, Singh B, Zhu Y. Anaerobic ammonium oxidation in agricultural soils-synthesis and prospective. Environ Pollut. 2019;244:127–34. https://doi.org/10.1016/j.envpol.2018.10.050.
70. Ostrom PH, DeCamp S, Gandhi H, Haslun J, Ostrom NE. The influence of tillage and fertilizer on the flux and source of nitrous oxide with reference to atmospheric variation using laser spectroscopy. Biogeochemistry. 2021;152:143–59. https://doi.org/10.1007/s10533-020-00742-y.
71. Corrochano M, Huérfano X, Menéndez S, Torralbo F, Fuertes T, Estavillo J, González C. Relationship between tillage management and DMPSA nitrification inhibitor efficiency. Sci Total Environ. 2020;718:134748. https://doi.org/10.1016/j.scitotenv.2019.134748.
72. Deng J, Wang G, Zhu Y, Zhou D, Zhou L, Yuan H, et al. Conventional tillage combined with residue removal reduces growing-season methane emissions in flooded paddy (Oryza sativa L. subsp. Japonica Kato) fields. Eur J Agron. 2022;140:126612. https://doi.org/10.1016/j.eja.2022.126612.
73. Angel R, Claus P, Conrad R. Methanogenic archaea are globally ubiquitous in aerated soils and become active under wet anoxic conditions. ISME J. 2012;6:847–62. https://doi.org/10.1038/ismej.2011.141.
74. Hornibrook ERC, Bowes HL, Culbert A, Gallego-Sala AV. Methanotrophy potential versus methane supply by pore water diffusion in peatlands. Biogeosciences. 2009;6:1491–504. https://doi.org/10.5194/bg-6-1491-2009.
75. Chistoserdova L, Vorholt JA, Lidstrom ME. A genomic view of methane oxidation by aerobic bacteria and anaerobic archaea. Genome Biol. 2005;6:208. https://doi.org/10.1186/gb-2005-6-2-208.
76. Conrad R. The global methane cycle: recent advances in understanding the microbial processes involved. Environ Microbiol Rep. 2009;1:285–92. https://doi.org/10.1111/j.1758-2229.2009.00038.x.
77. Baani M, Liesack W. Two isozymes of particulate methane monooxygenase with different methane oxidation kinetics are found in Methylocystis sp. strain SC2. Proc Natl Acad Sci USA. 2008;105:10203–8. https://doi.org/10.1073/pnas.0702643105.
78. Shen L-d, Ouyang L, Zhu Y, Trimmer M. Active pathways of anaerobic methane oxidation across contrasting riverbeds. ISME J. 2019;13:752–66. https://doi.org/10.1038/s41396-018-0302-y.
79. Kim S-Y, Kim E-K, Kwak JY, Moon HJ, Yoon JH. What to do with thyroid nodules showing benign cytology and BRAFV600E mutation? A study based on clinical and radiologic features using a highly sensitive analytic method. Surgery. 2015;157:354–61. https://doi.org/10.1016/j.surg.2014.09.003.

Publisher's note